Final Report

49p.

THE SCATTERING OF SHF RADIO WAVES BY HAIL AND WET SNOW

By: A. S. DENNIS

Prepared for:

NATIONAL AERONAUTICS AND SPACE ADMINISTRATION
WASHINGTON, D. C.

CONTRACT NASr-49(02)

STANFORD RESEARCH INSTITUTE

MENLO PARK, CALIFORNIA

*SRI

STANFORD RESEARCH INSTITUTE

MENLO PARK, CALIFORNIA

June 1964

Final Report

THE SCATTERING OF SHF RADIO WAVES BY HAIL AND WET SNOW

Prepared for:

NATIONAL AERONAUTICS AND SPACE ADMINISTRATION
WASHINGTON, D. C.

CONTRACT NASr-49(02)

By: A. S. DENNIS

SRI Project No. 3773

Approved: MYRON G. H. LIGDA, MANAGER
AEROPHYSICS LABORATORY

D. R. SCHEUCH, DIRECTOR
ELECTRONICS AND RADIO SCIENCES DIVISION

Copy No. 16

ABSTRACT

25763

Forward-scatter cross sections in hail and wet snow (which theoretically should exceed their back-scatter cross sections) have been derived from data recorded by Central Radio Propagation Laboratory in Colorado and by Stanford Research Institute in California.

Section II describes briefly the organization of the Colorado project, the equipment used, and the results of our preliminary analysis. Computed forward-scatter cross sections, which are averaged over several kilometers along the receiver beam, ranged up to $10^{-6.4}$ m^{-1} at 9.10 Gc and $10^{-8.1}$ m^{-1} at 4.86 Gc.

Section III describes the propagation path and the equipment used on the California project and presents a rather detailed discussion of the results. The most noteworthy findings are (1) that forward scatter by wet snow in the C-band region can exceed the back scatter by as much as 15 db, and (2) that the forward scatter from the melting layer contains a cross-polarized component which occasionally approaches the back scatter in the original plane of polarization. However, hail may have been present in the scattering volume when the cross-polarized component reached its maximum level.

The implications of these findings are discussed briefly in Sec. IV, but a complete assessment of their importance must await climatological studies of the frequency of the various precipitation forms and the heights to which the precipitation particles extend. Author

CONTENTS

ABSTRACT iii

LIST OF ILLUSTRATIONS vii

LIST OF TABLES ix

I INTRODUCTION 1

II SCATTERING BY SHOWERS AND THUNDERSTORMS IN COLORADO . . . 5

A. Project Organization 5

B. Geometry of Experiment 5

C. Preliminary Results 9

D. Evidence of Mie Scattering 11

III SCATTERING DURING WINTER STORMS IN CALIFORNIA 17

A. The Experimental Set-Up 17

B. Scattering Cross Sections as Functions of Observed Signals 20

C. Experimental Results 22

1. General Summary 22

2. Storm of 28-29 February 1964 23

3. Storm of 1 March 1964 24

4. Storm of 11-12 March 1964 25

5. Storm of 22-23 March 1964 30

6. Storm of 31 March-1 April 1964 31

D. Summary of Results 36

IV GENERAL DISCUSSION 37

ACKNOWLEDGMENTS 39

REFERENCES 41

ILLUSTRATIONS

Fig. 1 Back-Scatter Cross Section per Unit Volume as a Function of Frequency for Various Precipitation Rates 2

Fig. 2 Map Showing Typical Propagation Path, CRPL Precipitation-Scatter Experiment 6

Fig. 3 Ratio of Observed Scatter Cross Section at 9.10 Gc to That at 4.86 Gc, 1607-1619 MST, 27 June 1963 12

Fig. 4 Measured Values of $\eta_c L$, 1607-1619 MST, 27 June 1963 13

Fig. 5 Ratio of Actual Attenuation (by Scattering and Absorption) to That Given by the Rayleigh Approximation for Water at 18°C (after Gunn and East) 14

Fig. 6 Map Showing Propagation Path, SRI Precipitation-Scatter Experiment 18

Fig. 7 Cross-Section and Plan Views of Location of Common Volume, SRI Precipitation-Scatter Experiment 19

Fig. 8 Radar Pulses Scattered from Snow, 2213 PST, 1 March 1964 24

Fig. 9 Forward-Scatter Signals from Showers, 1140 PST, 1 April 1964 26

Fig. 10 Continuous Precipitation as Seen on PPI Radar Display, 2220 PST, 11 March 1964 27

Fig. 11 Calculated Cross Sections per Unit Volume, 11 March 1964. 28

Fig. 12 Forward-Scatter Signals from the Melting Layer, 2323 PST, 31 March 1964 (Antennas Fixed) 32

Fig. 13 Calculated Cross Sections per Unit Volume, 31 March-1 April 1964. 33

Fig. 14 Small Showers as Seen on PPI Radar Display, 1123 PST, 1 April 1964 35

TABLES

Table I Equipment Characteristics, CRPL Scatter Experiment. 8

Table II Operational Summary of SRI Precipitation-Scatter Experiment, 1964. 23

I INTRODUCTION

It was pointed out by Gordon in 1952 that scattering of radio waves by precipitation particles must be on occasion the dominant mechanism in radio propagation beyond the horizon at frequencies above some 300 Mc.[1]* Doherty and Stone[2] confirmed his prediction in a series of experiments during the late 1950's for radiation at 2.72 Gc.

Radio interference through the precipitation-scatter mode was overlooked in a report entitled "Frequency Allocations for Space Communications," which was issued by a Joint Technical Advisory Committee of the Institute of Radio Engineers and the Electronic Industries Association in 1961.[3] The oversight was pointed out in an SRI research memorandum prepared under the present contract in 1962, in which estimates were given of potential interference levels at ground stations monitoring satellite transmissions.[4] To check the estimates, a series of measurements was conducted using pulsed transmissions at 9.05 Gc toward a terrain-shielded receiver 5 km away.[5] Analysis of the observed signals yielded forward-scatter cross sections in rain compatible with those computed by previous authors by applying Rayleigh scattering theory to observed raindrop-size distributions.[6] This approach yields the following empirical formula:

$$\eta = (6.9 \times 10^{-12}) \, (f_{Gc})^4 R^{1.6} \qquad (1)$$

where η is the radar reflectivity, i.e., the back-scatter cross section per unit volume in reciprocal meters (square meters per cubic meter), f_{Gc} is the frequency of the incident radiation in gigacycles per second, and R is the rainfall rate in millimeters per hour. This function is shown graphically in Fig. 1, which is taken from Ref. 5. The relationship for snow included in the diagram is based on observations reported

*References are listed at the end of the report.

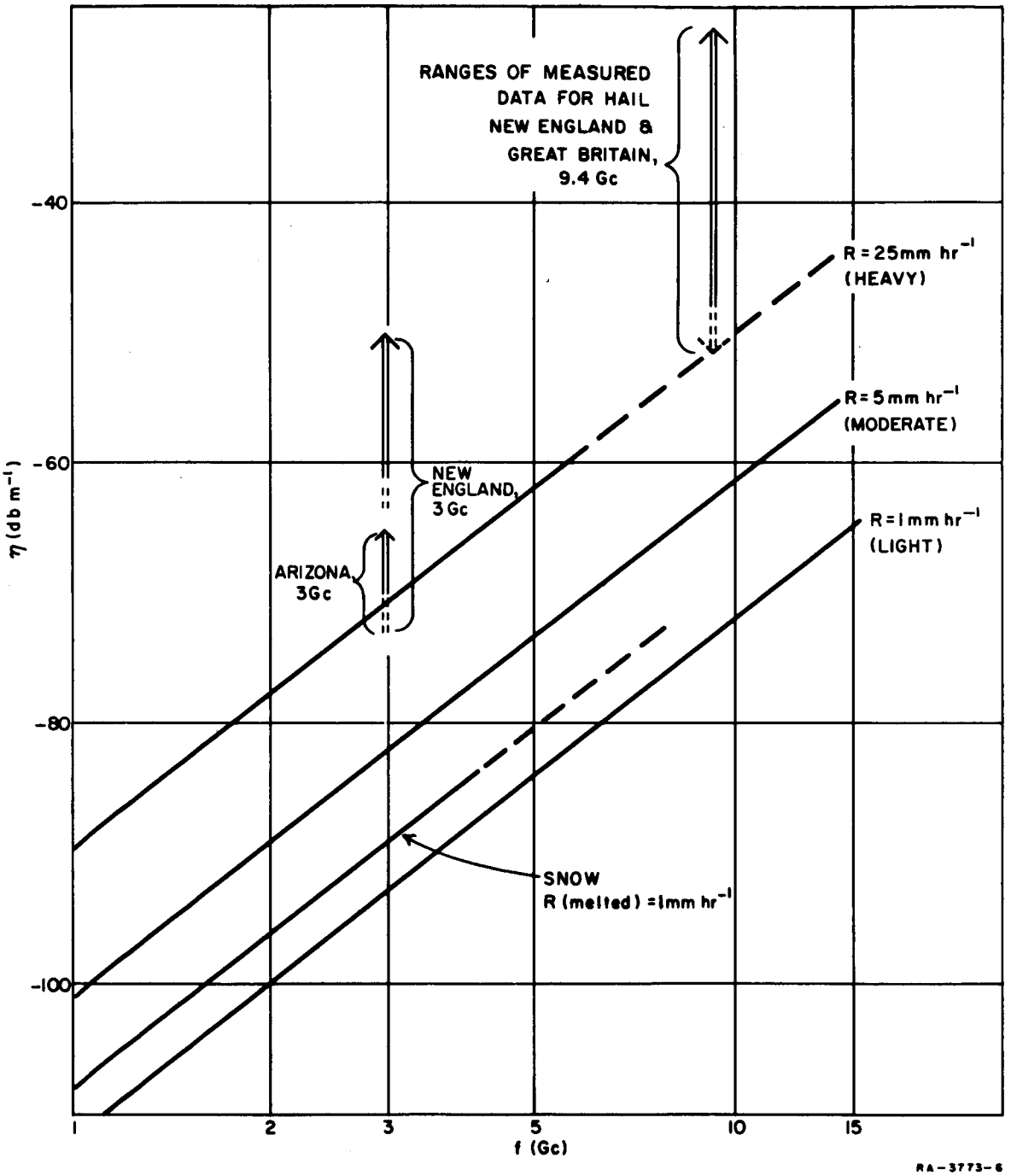

FIG. 1 BACK-SCATTER CROSS SECTION PER UNIT VOLUME AS A FUNCTION OF FREQUENCY FOR VARIOUS PRECIPITATION RATES

by Gunn and Marshall.[7] In practice, variations of several decibels occur in η at any given rainfall or snowfall rate because of variations in the particle size distribution.

The cross section of a Rayleigh scatterer varies as the sixth power of its diameter, so that precipitation characterized by large particles tends to produce strong radar echoes. The upper limit on raindrop diameter is about 5 mm. Snowflakes can grow somewhat larger, but the scattering efficiency of dry snowflakes is low because of their low density and the low dielectric constant of ice as compared with water. The largest radar returns, therefore, tend to occur with hail or wet snowflakes in the scattering volume.

The enhanced radar return from melting snow is known as the bright band, because of its appearance on range-height indicators. It usually extends downward about 400 meters from the 0°-C isotherm. Coalescence of wet snow crystals, accretion of cloud water, changes in fall speed, and the change in phase from water to ice all play a part in the bright-band phenomenon, but the relative importance of each has not been determined.[6,8] The maximum radar reflectivity in the bright band occurs near the lower edge, and is typically 4 to 8 times greater than the reflectivity in the rain beneath. The bright band is most pronounced in stable weather situations with widespread precipitation. In showers and thunderstorms, where high concentrations of super-cooled water are common above the 0°-C level, it is sometimes entirely absent.

The effects associated with wet snowflakes and hailstones go beyond increased back scattering. The Rayleigh approximation breaks down when the particle diameter becomes comparable to the radar wavelength, and the complete Mie scattering theory must be applied.[6] Computations of scatter cross sections for large ice spheres using the Mie theory show that they sometimes scatter more strongly forward than backward, with the ratio of the forward-scatter to the back-scatter cross section running as high as 100 or more.[9] The results of other writers, including Gunn and East,[6] show that spherical water drops also scatter forward more strongly than backward when their diameters are comparable to the

wavelength. It is reasonable to anticipate similar behavior for large, wet snowflakes, although the scattering patterns of large nonspherical particles are so complex that no exact computations for them have yet been possible.

Small nonspherical particles have been considered by Atlas et al.[10] They conclude that dry snowflakes behave almost like small spheres, which return linearly polarized radiation without any change in polarization, but that wet snowflakes would produce a significant cross-polarized return. However, experimental results given by Newell et al.[11] and by Wexler[12] show that some cross-polarized signal is present in returns from dry snow, although the depolarization effect is less pronounced than in wet snow. In the bright band, the cross-polarized return can be as little as 10 db below the component in the original plane of polarization.

The scattering of SHF radio waves by various types of precipitation has been studied under this contract, with particular attention to hail and wet snow. Section II presents a preliminary analysis of scattering from showers of rain and hail, recorded by the Central Radio Propagation Laboratory in Colorado during the early summer of 1963. Section III discusses the recording and analysis of scatter signals during winter storms of the 1963-64 season in California. The California part was proposed first, in an SRI Proposal for Research entitled "Measurements of Forward Scatter in Precipitation at 6.0 Gc," which was submitted to NASA in December 1962. The Colorado analysis was suggested in an addendum to the original proposal, submitted in May 1963.

Both phases of the work were funded under an extension of Contract NASr-49(02) between NASA and SRI, since the proposed work fell within the contract's original objective, namely, to determine conditions for the multiple use of frequency allocations for satellite communications and ground services. The work done under the contract up to the end of 1962 was summarized in an earlier report to the sponsor.[13] The precipitation-scatter investigations represent the entire effort under the contract since then, so that this report and Ref. 13 together cover all of the work done under the contract.

II SCATTERING BY SHOWERS AND THUNDERSTORMS IN COLORADO

A. PROJECT ORGANIZATION

In order to obtain data useful in predicting interference levels due to showers and thunderstorms, the Central Radio Propagation Laboratory of the National Bureau of Standards is conducting a program to measure precipitation scatter in northeastern Colorado, under a contract with the National Aeronautics and Space Administration. In particular, the program is intended to measure scattering by storms producing hail. Measurements are being made at 4.86 Gc (C band) and at 9.10 Gc (X band), with the transmitters at Akron, Colorado, and the receivers 170 km away at Table Mesa (Fig. 2). The scatter signals are recorded simultaneously on magnetic tape and on a Sanborn recorder. In this work, the Central Radio Propagation Laboratory maintains close cooperation with Colorado State University personnel who are studying hailstorms in the same general area. Data provided to the Laboratory by Colorado State University include records from a weather radar set operated at New Raymer (Fig. 2) by Atmospherics, Inc., as part of the University's program.

A preliminary analysis of some of the records obtained in the CRPL program constituted part of the work done at SRI under the present contract. Duplicate recordings from the Sanborn machine and time-lapse motion pictures of the New Raymer weather radar screen were used in this work. The results of the analysis were submitted to NASA in a research memorandum[14] in October of 1963. The following is a resumé of the more significant findings.

B. GEOMETRY OF EXPERIMENT

The CRPL forward-scatter experiment uses low-gain transmitting antennas to illuminate entire showers (or groups of showers) with continuous-wave radiation, and scans the illuminated regions with very high-gain receiving antennas. For this situation, the beam geometry

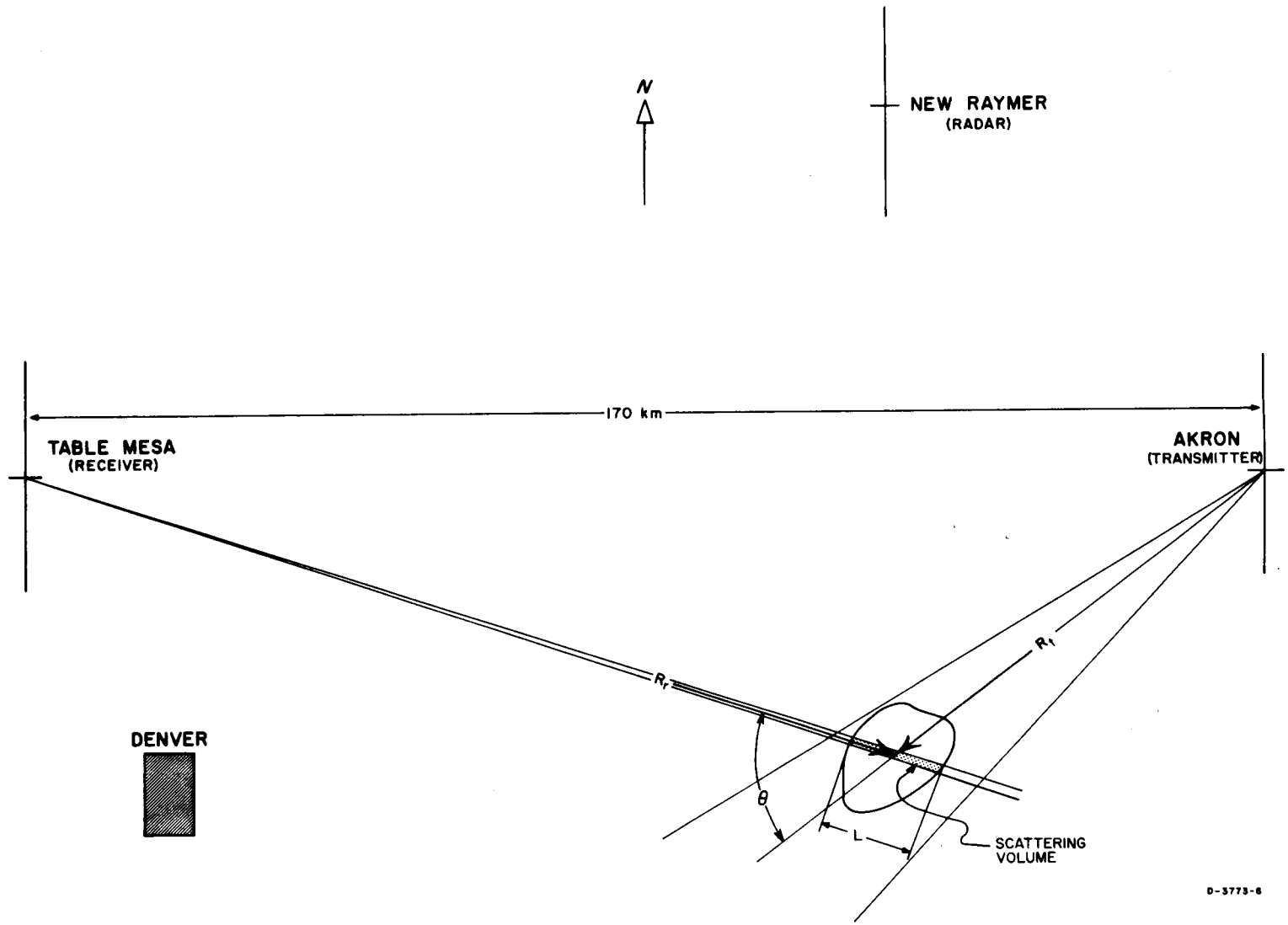

FIG. 2 MAP SHOWING TYPICAL PROPAGATION PATH, CRPL PRECIPITATION-SCATTER EXPERIMENT

is rather simple (Fig. 2); theoretically, the common volume can be considered to include all of the receiver beam between the half-power points of the transmitter beam. Usually, however, the length of the contributing region (along the receiver beam) is restricted further by the dimensions of the shower causing the scattering. For such a case, Eq. (12) of Ref. 4 can be adapted to the form

$$P_r = \frac{P_t G_t}{4\pi R_t^2} \cdot \eta V \cdot \frac{G_r \lambda^2}{(4\pi R_r)^2} \qquad (2)$$

where

P_r is the (mean) received power
P_t is the transmitted power
G_t is the gain of the transmitting antenna
η is the scatter cross section per unit volume for scattering in the direction of the receiver, averaged over that part of the shower in the receiver beam
V is the volume contributing to the received power
G_r is the gain of the receiving antenna
λ is the wavelength of the radiation
R_t is the range of the shower from the transmitter, and
R_r is the range of the shower from the receiver.

Upon rearrangement, this yields

$$\eta V = \frac{(4\pi)^3 R_t^2 R_r^2 P_r}{\lambda^2 G_t G_r P_t} \quad . \qquad (3)$$

In the present case, we can write

$$V = L \cdot \frac{4\pi R_r^2}{G_r} \qquad (4)$$

where L is the length the shower extends along the receiver beam. Substitution of this in Eq. (3) leads to

$$\eta L = \frac{(4\pi)^2 R_t^2 \cdot P_r}{\lambda^2 G_t \cdot P_t} \quad . \qquad (5)$$

As η has dimensions of reciprocal length (area per unit volume), ηL is a pure number.

The equipment characteristics for the present experiment are shown in Table I.

Table I

EQUIPMENT CHARACTERISTICS, CRPL SCATTER EXPERIMENT

	X Band	C Band
f (Gc)	9.10	4.86
λ (cm)	3.3	6.2
P_t (watts)	1000	1000
G_t (db)	22	25
G_r (db)	60	56

The receiver beamwidths are approximately 15 minutes at X band and 30 minutes at C band. At a range of say, 100 km, the C-band receiver beam is only 0.9 km wide, well under the diameter of a typical shower. We can assume, therefore, that L is the same for the two frequencies, and use the following simple formula:

$$\frac{\eta_x}{\eta_c} = \frac{P_{rx}\lambda_c^2 G_{tc} P_{tc}}{P_{rc}\lambda_c^2 G_{tx} P_{tx}} \qquad (6)$$

where all symbols are as defined previously, apart from the addition of the subscripts x and c. Substituting numerical values from Table I, we find

$$\frac{\eta_x}{\eta_c} = 10^{0.8}\,\frac{P_{rx}}{P_{rc}} \quad . \qquad (7)$$

The CRPL equipment operates in very narrow frequency bands, 500 cps wide for the X-band system and 1,200 cps wide for the C band. These are comparable to the Doppler shifts associated with the motions of precipitation particles. As the combined elevation angles of the transmitter

and receiver beams never exceeded 6°, the Doppler shift for storms off the direct path can be estimated from the horizontal wind, neglecting particle fall velocities and vertical currents. Let s_T and s_R be unit vectors directed from the shower toward the transmitter and receiver, respectively, and let **V** be the wind vector in the part of the shower contributing to the scattered signal. Then the Doppler shift of the signal produced by a particle moving with the wind is given by

$$\Delta f = \frac{1}{\lambda} [s_T \cdot \mathbf{V} + s_R \cdot \mathbf{V}] \quad . \tag{8}$$

In some of the cases studied, the Δf computed for the X-band system was comparable to the 500-cps bandwidth, so that signal is likely to have been lost occasionally through being shifted out of the receiver pass band. At C band, the shifts are smaller and the pass band wider; no cases were found where this effect would be serious.

C. PRELIMINARY RESULTS

The records chosen for analysis were obtained on 14, 26, and 27 June 1963. On 26 and 27 June, vertical polarization was used at the transmitters and receivers, so that, for scatterers off the Great Circle path, the scattered component perpendicular to the observation plane was recorded. Thus the scatter signals were contributed by the i_1 term of the Mie scattering theory.[9] For the special case of Rayleigh scattering ($\alpha = 2\pi\, a/\lambda \ll 1$, where a is the particle radius), i_1 is independent of the scattering angle, θ. On 14 June horizontal polarization was used, so that, for scatterers off the Great Circle path, the component parallel to the scattering plane was observed. The signals observed in this case are contributed by the i_2 term of the Mie theory, which vanishes for Rayleigh scatterers at $\theta = \pi/2$. However, most of the 14 June observations were made with θ near 30°, where i_2 is not much smaller than i_1.

On 26 and 27 June, some observations were made with the antennas directed toward each other in azimuth. In this case, the observation plane is vertical and the response is in the i_2 term, rather than the

i_1 term. However, as i_1 and i_2 are defined relative to the observation plane, this switch merely serves to maintain the original polarization (vertical in this case).

The strongest signals observed during the three days were -97 dbm at X band and -103 dbm at C band. On 27 June, some observations of the tropospheric scatter signal were made with the beams directed at each other; the observed signals averaged -113 dbm at X band and -118 dbm at C band. Thus, the precipitation scatter signals from the isolated showers ran as much as 15 db above the troposcatter signal on the direct path.

The function (ηL) has been computed as described above for those cases where the radar showed showers in the common volume of the transmitter and receiver beams. The maximum values, -26 db at X band and -43 db at C band, occurred in a shower observed at 1548 MST on 27 June, 90 km from the receiver site on a bearing of 117 degrees. In this case, L was 6 km; hence η_x and η_c were -64 db m^{-1} and -81 db m^{-1}, respectively.

If one were to assume that the precipitation particles were Rayleigh scatterers, following previously observed typical raindrop-size distributions, one could deduce a rainfall rate of 4 mm/hr on the basis of the X-band observation, but only 2 mm/hr on the basis of the C-band observation (Fig. 1). This discrepancy is apparently due to non-Rayleigh scattering at the X-band frequency.

The data provided contain 18 cases where it is possible to compute ηL and the average value of η with the receiver beam passing through the core of a precipitation cell. The geometric average of η_x, that is, the average of the individual cases expressed on a decibel scale, is -70 db m^{-1}; the geometric average of η_c over the 18 cases is -88 db m^{-1}.

This average value of η_c corresponds to a rainfall rate of the order of 0.5 mm/hr, which is quite low. However, there is a tendency for rainfall rates in showers to increase sharply with increasing penetration toward the center. Therefore, one would expect rainfall rates near the centers to exceed the computed values, which are averages along a diameter, by a considerable margin.

D. EVIDENCE OF MIE SCATTERING

As the Rayleigh scatter cross section varies as f^4, the ratio η_x/η_c for Rayleigh scatterers in the present study is 11 db. The observed values of the ratio range from 10 to 25 db, so that the ratio for Rayleigh scatterers serves as a lower bound, within the limits of measurement error. It is possible that the X-band signal was reduced on occasion by as much as 3 db by Doppler effects, but no attempt to correct for this effect is made in this section.

Attempts have been made to correlate the ratio η_x/η_c with the scattering angle Θ, with the height of the contributing region, and with η_c. The ratio does not show a significant correlation with any of the three parameters. Since attenuation is more important at X band than at C band, the records have been examined to see if the low values of the ratio are associated with contributing regions shielded from the transmitter or receiver by intervening showers. No evidence of such an effect has been found, and the low average rainfall rates derived above indicate that attenuation is of minor importance in the small showers under consideration.

The variations in the ratio η_x/η_c are real and systematic, however. This is clearly seen in Fig. 3, which shows the measured ratio as a function of receiver bearing and elevation of the contributing region between 1607 and 1619 MST on 27 June. The reflectivity at C band in the same region is shown in Fig. 4; comparison of Figs. 3 and 4 shows that the maximum of η_x/η_c does not coincide with the shower core as shown by η_c. Of particular significance is the fact that the ratio is a maximum some 4 km above ground, whereas η_c reaches its maximum close to or at the ground.

The ratios shown in Fig. 3 can be explained logically on the basis of figures presented by Herman and Battan[9] and by Gunn and East.[6] Herman and Battan have computed the Mie scattering functions, $i_1(\Theta)$ and $i_2(\Theta)$, for ice spheres for various values of α ($= 2\pi a/\lambda$, where a is the particle radius) up to 5. Their results are computed for the

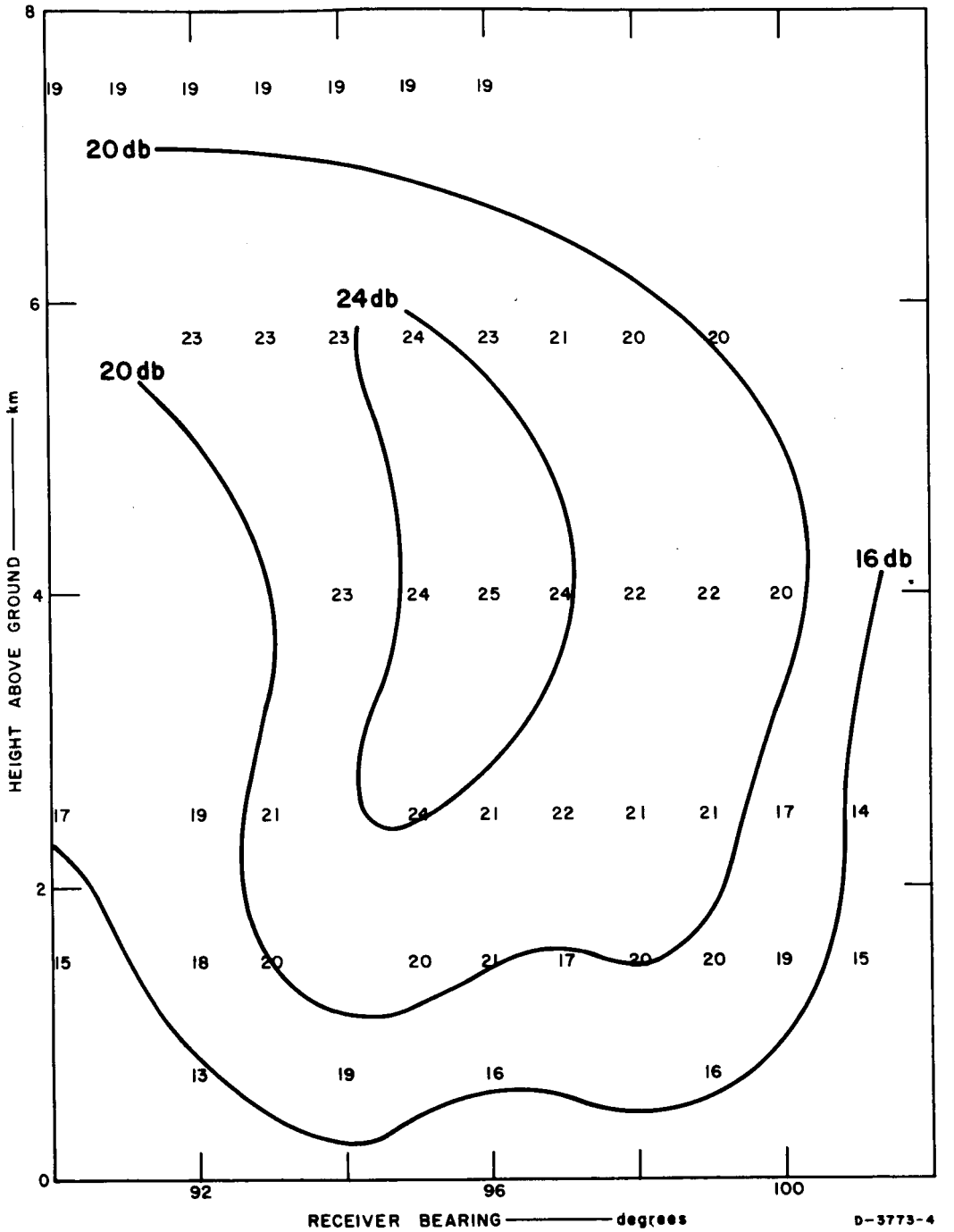

FIG. 3 RATIO OF OBSERVED SCATTER CROSS SECTION AT 9.10 Gc TO THAT AT 4.86 Gc, 1607-1619 MST, 27 JUNE 1963

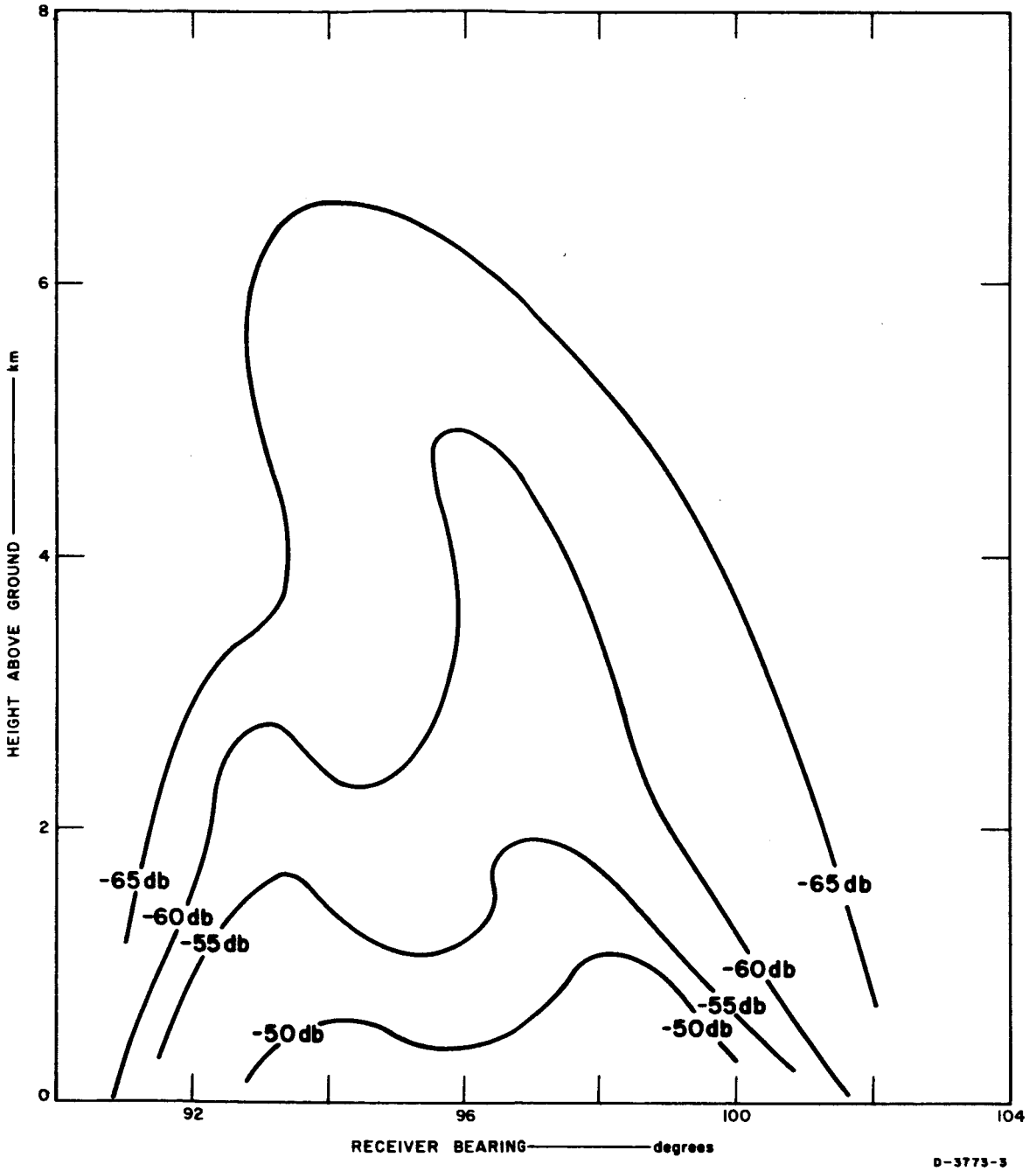

FIG. 4 MEASURED VALUES OF $\eta_c L$, 1607-1619 MST, 27 JUNE 1963

wavelength 3.2 cm, but should be applicable at C band as well, since the refractive index of ice is independent of frequency in the microwave region.[6] Angular scattering functions for water drops in the microwave region are not available. However, it appears that the relative efficiency of scattering in a given direction at two different frequencies can be estimated from Fig. 5, which is reproduced from Gunn and East. This figure shows the ratio of Q_t (Mie), the total Mie cross section (scattering plus absorption), to Q_t (Rayleigh), the total Rayleigh cross section, for water drops at 18°C at several frequencies

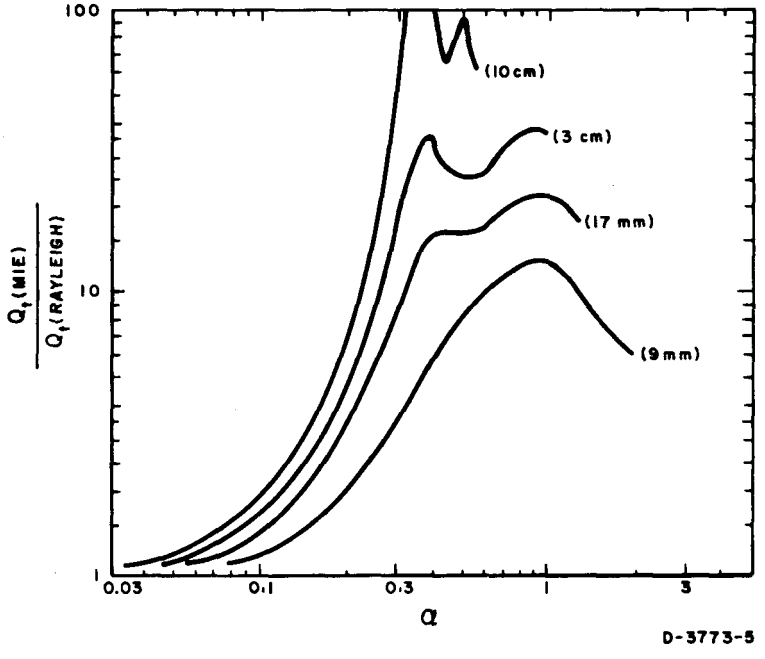

FIG. 5 RATIO OF ACTUAL ATTENUATION (by scattering and absorption) TO THAT GIVEN BY THE RAYLEIGH APPROXIMATION FOR WATER AT 18°C (after Gunn and East)

in the microwave region. Figure 9 of Ref. 9 shows that the fraction of the total scattering contained in the cones defined by $\theta < 10^\circ$, $\theta < 20^\circ$, and so on, is a slowly varying function of α. Therefore, we will make use of Fig. 5 in estimating the ratio η_x/η_c for raindrops.

From Fig. 5, it is found that the maximum possible η_x/η_c for raindrops occurs for drops of 3- to 4-mm diameter. In this range, the

ratio of Q_t (Mie) to Q_t (Rayleigh) is approximately six times (8 db) larger at 9.1 Gc than it is at 4.86 Gc. By adding in the 11-db difference for Rayleigh scatterers, it is found that η_x/η_c cannot exceed 19 or 20 db if the scatterers are raindrops, or are wet spherical hailstones whose scattering properties resemble those of raindrops.

Herman and Battan's results[9] on ice spheres show that the most rapid increase of forward-scatter cross section with α occurs somewhere in the range $0.5 < \alpha < 1.5$. The function $i_1(\theta)$ for $\theta < 10^\circ$ is about 32 db larger at $\alpha = 1.5$ than at $\alpha = 0.5$. This function must be weighted by λ^2 to obtain the scatter cross sections. In the present case, $(\lambda_c/\lambda_x)^2$ is near 5 db, leaving 27 db as the ratio of the forward-scatter cross sections at $\alpha = 1.5$ and $\alpha = 0.5$. In the present case, the ratio of α at X band to that at C band is nearer 2 than 3. Unfortunately, the functions for $\alpha = 1.0$ are not presented in Ref. 9; it appears likely, however, that the 27-db range is concentrated in the upper part of the range of α, rather than being uniformly distributed between 0.5 and 1.5. Therefore, it is most likely that the observed cases with η_x/η_c in excess of 20 db are due to dry hail with α near 1.5 at X band and 0.8 at C band; that is, hail with the greater part of the signal contributed by stones having diameters near 15 mm. This is consistent with the data of Fig. 4, where the maximum value of η_x/η_c is shown at 4 km above ground, well above the melting level. It is possible that shape effects play a part here also, but they cannot be assessed accurately as the Mie functions have not been generalized to large nonspherical particles. Studies of back-scattering by small ellipsoids show that significant effects could occur.

The decrease in η_x/η_c toward the top of the storm can be attributed to a preponderance of fine hailstones or snow crystals or both; the decrease in η_x/η_c downward from the 4-km level can be attributed to a preponderance of liquid water in the lower part of the shower. It is interesting to note the approach to Rayleigh scattering near the lower edges, where relatively small raindrops are ordinarily encountered. From Fig. 5, it would appear that drop diameters there are 1 to 2 mm.

As small water drops are more efficient scatterers than ice spheres of the same size, the increase in reflectivity at C band with decreasing height can be attributed to the melting of hailstones to raindrops. The downward indentation of the -60-db contour on Fig. 4 coincides with the downward extension of the -24-db contour on Fig. 3; it may be associated with a shaft of falling hail, with the stones not showing appreciable melting until close to the ground.

Thunderstorm activity in northeastern Colorado appears to have been lighter than usual during the summer of 1963. No measurements have been obtained to date on storms producing significant hail at the ground. The observations by CRPL are to be continued during the 1964 thunderstorm season in the hopes of obtaining records during such storms.

III SCATTERING DURING WINTER STORMS IN CALIFORNIA

A. THE EXPERIMENTAL SET-UP

The main objective of this experiment was to determine forward-scatter cross sections in the bright band. The requirements in choosing the propagation path were, first, that the transmitter and receiver beams should intersect at a small angle near the 0°C isotherm and, second, that the receiving antenna be shielded from the transmitter by the terrain to eliminate side-lobe effects. A suitable path, 17.6 km long, was found near Sonora, California, in the western foothills of the Sierra Nevada (Fig. 6).

The transmitter was located on a small ridge near the town of Tuolumne at an elevation of 860 m. The site chosen for the remote receiver was Columbia Airport, on a bearing of 291° true from the transmitter, at an elevation of 660 m. Due to small foreground ridges, the horizon angles at the transmitter and remote-receiver sites were 2° and 3.5°, respectively. A plan view showing the location of the common volume with the antennas directed toward each other is shown in Fig. 7(a), with beamwidths as given below. The path profile is shown in Fig. 7(b). The presence of the two ridges on the path ruled out not only direct propagation but also propagation through knife-edge diffraction.

The experiment was conducted with C-band equipment, which is the frequency band used by those communications satellites launched to date.

A complete C-band weather radar set was operated at the transmitter site. It served two purposes: to provide information on precipitation patterns in the immediate area, and to supply the signals for the scatter cross-section determinations. The radar was supplied by the U.S. Air Force from a surplus AMQ-15 weather system. The set transmitted 5.90-Gc pulses of 3 μsec duration and 250 kw peak power at a pulse repetition frequency of 333 per second. It had a pencil beam, with the width to the half-power points specified as 3.5°, and an

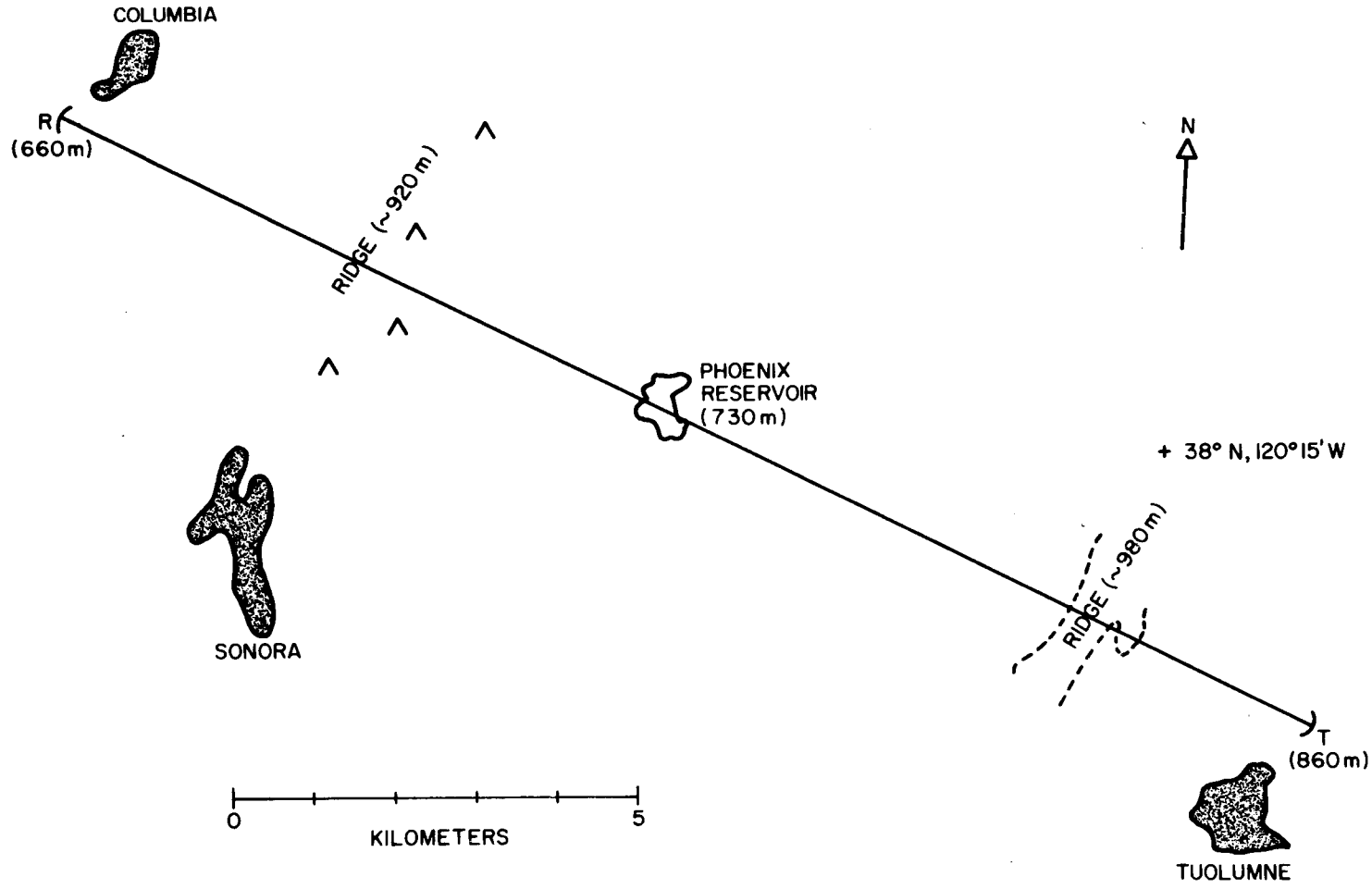

FIG. 6 MAP SHOWING PROPAGATION PATH, SRI PRECIPITATION-SCATTER EXPERIMENT

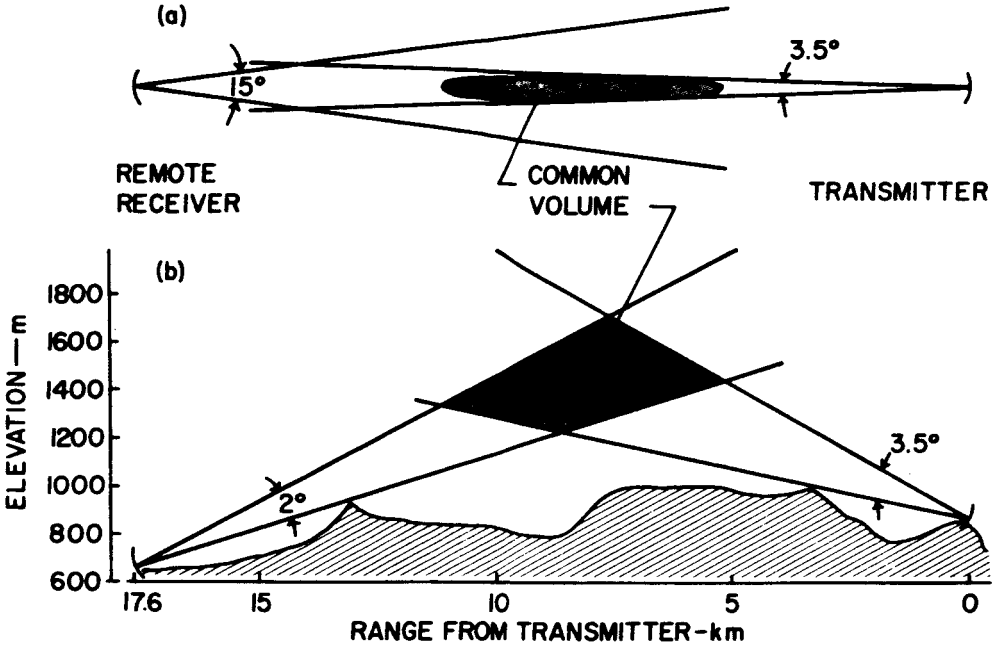

FIG. 7 CROSS-SECTION AND PLAN VIEWS OF LOCATION OF COMMON VOLUME, SRI PRECIPITATION-SCATTER EXPERIMENT

effective gain of 34 db, which corresponds to an effective aperture of 0.5 m^2. The antenna elevation was set so that the lower edge of the beam, measured to the half-power point, was directed at the horizon when pointed toward the remote receiver.

Considerable effort was spent in overhauling and modifying the radar set before it was moved to the site in February of 1964. It was mounted on a trailer for easier transport. A flexguide section was inserted into the antenna circuit to permit changes in polarization. A VD-2 display unit was added to permit photography at times when the set was operated in the plan-position-indicator mode. While the photographic records are useful in locating precipitation areas, they do not provide more than crude estimates of signal amplitude. Therefore, an A-scope was added during the course of the project to permit measurements of the signals back-scattered from the common volume.

The remote receiver was taken from an incomplete SG-6B radar obtained from Mare Island Naval Shipyard. This equipment normally operates

in the frequency range 6.2 to 6.6 Gc, but proved capable of modification to 5.9 Gc. The SG-6B, being a marine radar, was designed to have a beam sharp in azimuth but broad in the vertical. The rated antenna gain was 29 db. For the experiment, the antenna was mounted on its side, yielding a beam 15° wide in azimuth and 2° in height. This was done to obtain a beam whose height at the range of the common volume would approximate the depth of the bright band, which is usually in the range 300-500 m (Ref. 8). With this arrangement, the antenna was sensitive to vertically polarized radiation.

The receiver was set up in a small building at Columbia Airport, with the antenna on the roof directed at the transmitter site, and the lower edge of the beam, measured to the half-power point, directed at the horizon. The antenna remained fixed throughout the experiment. An oscilloscope display of the receiver output was photographed for subsequent analysis, with a second oscilloscope serving as a monitor unit.

The radar receiver and the remote receiver were calibrated on the site during the course of the experiment. This was done by feeding known signals from a test set into the receiver being tested and noting the amplitude (in volts) of the output. This procedure was carried out for four different gain settings of the remote receiver, to provide a wide dynamic range. The losses in the coaxial cable used at the remote receiver were also measured using the test equipment; allowance for them has been made in analyzing the data.

B. SCATTERING CROSS SECTIONS AS FUNCTIONS OF OBSERVED SIGNALS

To compare the forward-scatter and the back-scatter cross sections per unit volume in the region common to the transmitter and receiver beams, it is necessary to examine the path geometry, and to derive expressions for the cross sections in terms of the signals recorded at the radar site and at the remote receiver.

The back-scatter cross section per unit volume, η_b, in the common volume can be derived using the weather radar equation[6] which yields,

upon rearrangement,

$$\eta_b = \frac{8\pi R_t^2 \overline{P}_r}{P_t A_e h} \tag{9}$$

where

R_t is the range from the transmitter to the contributing region
$\overline{P}_r$ is the mean received power at the radar
P_t is the peak transmitter power
A_e is the effective antenna aperture, and
h is the length of a pulse in space.

The length h is given by $c\tau$, where c is the speed of light and τ is the pulse duration.

Reference to Fig. 7 shows that R_t is approximately 8.8 km near the middle of the common volume. The other fixed parameters are P_t = 250 kw, A_e = 0.5 m^2, and h = 900 m. Substitution of these values leads to

$$\eta_b = \overline{P}_r + 12 \quad , \tag{10}$$

where η_b is expressed in decibels with respect to 1 reciprocal meter and $\overline{P}_r$ is expressed in decibels with respect to 1 watt. (The use of $\overline{P}_r$, rather than an instantaneous value, is necessary because of the fluctuating nature of the signal from random scatterers such as precipitation particles.)[15]

In order to compute η_f, the forward-scatter cross section as seen from the remote receiver, it is necessary to find V, the common volume.* The receiver beam is very broad and flat, so that the common volume can be considered as the difference between two conical frustrums cut from the transmitter beam by the top and bottom of the receiver beam. This treatment yields 0.5 km^3 as the value of V. In some cases, only part

---

*η_f is comparable to, but not identical with, the η_c of Sec. II.

of the common volume is filled with precipitation; a correction factor must then be applied. Using Eq. (2), with $V = 0.5\ km^3$, $R_t = R_r = 8.8$ km, and all other parameters as previously given, leads to

$$\eta_f = \overline{P}_{rr} + 13 \qquad (11)$$

where $\overline{P}_{rr}$ denotes the mean power collected in the antenna of the remote receiver, and the units are the same as those used in Eq. (10).

C. EXPERIMENTAL RESULTS

1. General Summary

The equipment used on the project was left in position from 19 February to 9 April 1964. It was operated during five storms by personnel who traveled from Menlo Park to the field sites for that purpose. The five storms sampled included all the major precipitation occurrences in the Sonora area of the Sierra Nevada during the seven weeks of operation. Only minor trouble was experienced with the electrical and electronic equipment, in spite of its being unattended between storms.

In addition to the observations described below, observations were made at Menlo Park during a storm in January of 1964 to check out the equipment, and the equipment was operated on the sites under fair-weather conditions on a number of occasions. No signals were ever observed without precipitation in the common volume.

In analyzing the results, η_b and η_f have been computed from the observed values of $\overline{P}_r$ and $\overline{P}_{rr}$ in accordance with Eqs. (9) and (10), respectively. The values of η_f represent an average over a larger volume than do the values of η_b presented. The radar records are of great assistance in determining which variations in the ratio η_f/η_b correspond to real changes in the scattering pattern and which are due to the difference in the volumes sampled. Weather data obtained from the U.S. Weather Bureau have been used in interpreting the observations, particularly in establishing the height of the melting layer.

The results for the five storms sampled are summarized in Table II. Detailed discussions for all of them are given in chronological order in the following subsections.

Table II

OPERATIONAL SUMMARY OF

SRI PRECIPITATION-SCATTER EXPERIMENT, 1964

Storm	Precipitation in Common Volume	Transmitter* Polarization	Remarks
28-29 February	None (showers in vicinity)	Vertical	No signals
1 March	Dry snow	Vertical	Signal recorded, η_f around 10^{-8} m^{-1}
11-12 March	Wet snow changing to dry	Vertical	η_f equalled or exceeded η_b.
		Horizontal	Forward-scatter signal too weak to measure
22-23 March	Dry snow	Vertical	η_f in range 10^{-7} to 10^{-8} m^{-1}
		Horizontal	η_f around 10^{-10} m^{-1} (Receiver performance improved)
31 March-1 April	Wet snow and rain, then wet snow and (possibly) hail	Vertical	η_f up to 10^{-7} m^{-1} on occasion, exceeding η_b by 6-18 db.
		Horizontal	η_f as high as 10^{-8} m^{-1}, nearly equal to η_b

*Receiver polarization vertical at all times.

2. Storm of 28-29 February 1964

Light showers occurred in the Sonora area on the evening of 28 February, accompanying and following a weak front moving eastward through California. The radar was operated from 2000 to 2045 PST and again from 2245 until 0130 PST of 29 February. The remote receiver was turned on for a time, but no showers moved through the common volume while it was in operation. No forward-scatter signals were seen.

3. Storm of 1 March 1964

A more extensive storm with widespread rain and snow moved into the Sierra Nevada on 1 March. The heaviest precipitation in the Sonora area fell around 2000 PST, and apparently coincided with the passage of a front. The melting level ahead of the front was about 1.8 km above sea level. As it turned out, no forward-scatter signals were recorded before 2130 PST. It is estimated that the 0°C isotherm had by then dropped to about 1.2 km above sea level, as the rain had turned to snow on the ridges along the path. Thus, all the forward-scatter signals recorded were from dry snow. At the end of the storm, around midnight, snow was accumulating on the ground at the transmitter site, at 860-m elevation.

The radar set was turned on, with vertical polarization, at 1400 PST. The remote receiver was placed in operation at 1500 PST, but the forward-scatter signals could not be identified. The equipment was turned off at 1725 PST. Before a second run was attempted, the coaxial cable leading to the antenna was shortened. With this improvement, it was possible to identify the radar pulses when the receiver was placed in operation again at 2130 PST.

A sample of the results is shown in Fig. 8. The oscilloscope was running on external trigger with the writing speed at 1 msec/cm.

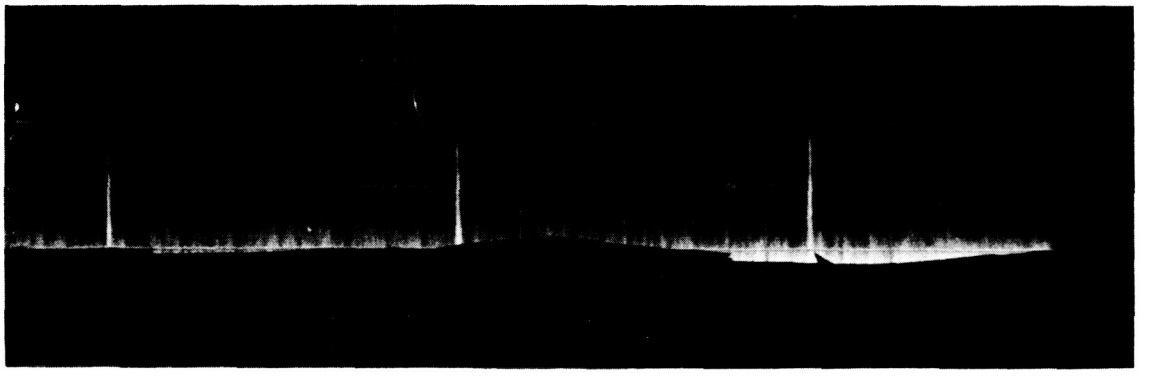

FIG. 8 RADAR PULSES SCATTERED FROM SNOW, 2213 PST, 1 MARCH 1964

The radar was scanning, sweeping its beam through the receiver beam once every 8 seconds. The camera trigger was set to advance the film after each scan, but it had some lag. Each picture undoubtedly represents several oscilloscope sweeps, so that each spike represents the strongest of an undetermined number of pulses.

The forward-scatter cross section in the common volume, η_f, computed for individual spikes between 2213 and 2231 PST, ranges from -89 to -82 db m^{-1}. The corresponding radar records show a broad band of light precipitation with some striations moving through the common volume. Comparison of the values of η_f with Fig. 1 shows them to be typical for η_b in light snow, where η_f and η_b would be expected to be equal.

At 2230 PST, the sweep speed of the oscilloscope display at the remote receiver was changed to 1 sec/cm. At this speed, the individual pulses are not resolved. Each scan of the transmitter is shown as one or more sharp wedges (see Fig. 9, from a photograph made on 1 April). Variations in amplitude are apparent, but it is not always possible to state which are due to variations in precipitation rate across the broad receiver beam and which are due to chance fluctuations of the incoherent signal. The peak amplitudes observed between 2231 and 2300 PST correspond to values of η_f ranging from -81 to -76 db m^{-1}. The radar photographs indicate steady light precipitation (presumably snow) in the common volume during this period. It is likely that the higher signals recorded after 2230 PST are due to the difference in the recording method, rather than to a true increase in η_f.

4. Storm of 11-12 March 1964

This storm, which began late on 11 March and lasted into the following day, was characterized by low temperatures and very persistent, uniform precipitation, illustrated in Fig. 10 (a photograph of the radar screen taken at 2220 PST on 11 March). The V-shaped notches in the precipitation echoes are shadows of nearby peaks; apart from them, little variation with angle is apparent in the pattern.

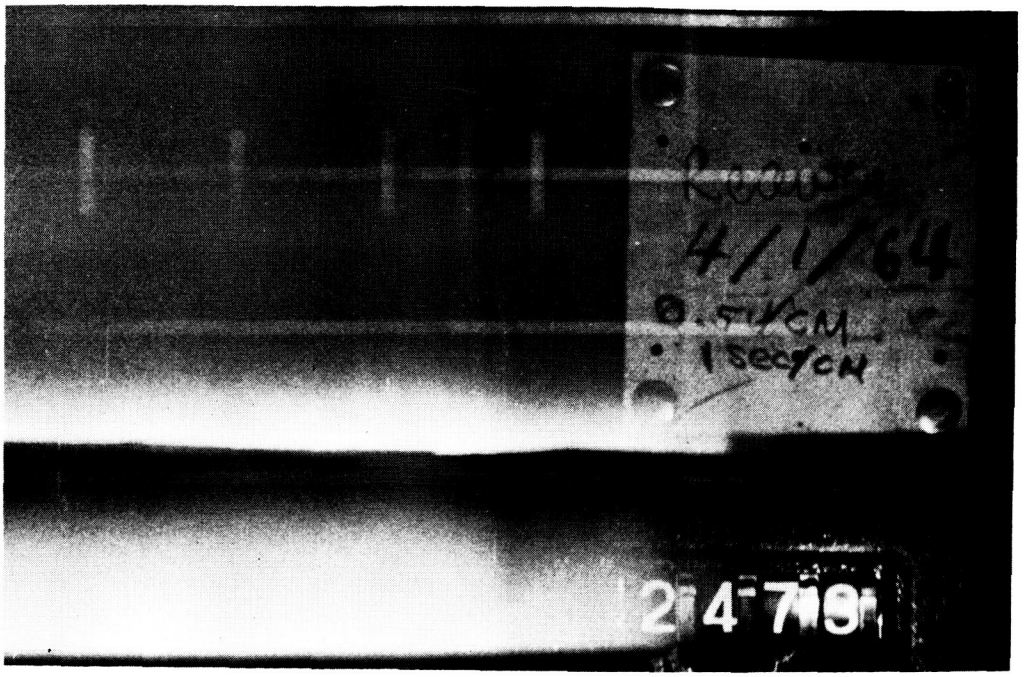

FIG. 9 FORWARD-SCATTER SIGNALS FROM SHOWERS, 1140 PST, 1 APRIL 1964

Uniform echo, apart from minor striations and a pebbling due to the incoherent nature of the back-scattered signal, extends out to the range at which the beam rises above the detectable precipitation.

The weather data available indicate that the 0°-C level was about 1.4 km above sea level during the evening and dropped slowly during the night. Wet snow must have been present in the lower part of the common volume during the first part of the storm.

The transmitter was operated with both vertical and horizontal polarization during the storm. The transmitting antenna was occasionally pointed directly at the remote receiver in an attempt to obtain photographic records suitable for statistical analysis on a pulse-by-pulse basis. Unfortunately, the photographs of the oscilloscope at the receiver site were too far underexposed to be of use.

The results for the evening of 11 March are summarized in Fig. 11. The forward-scatter cross sections are based on observations of the monitor scope at the remote-receiver site. The back-scatter

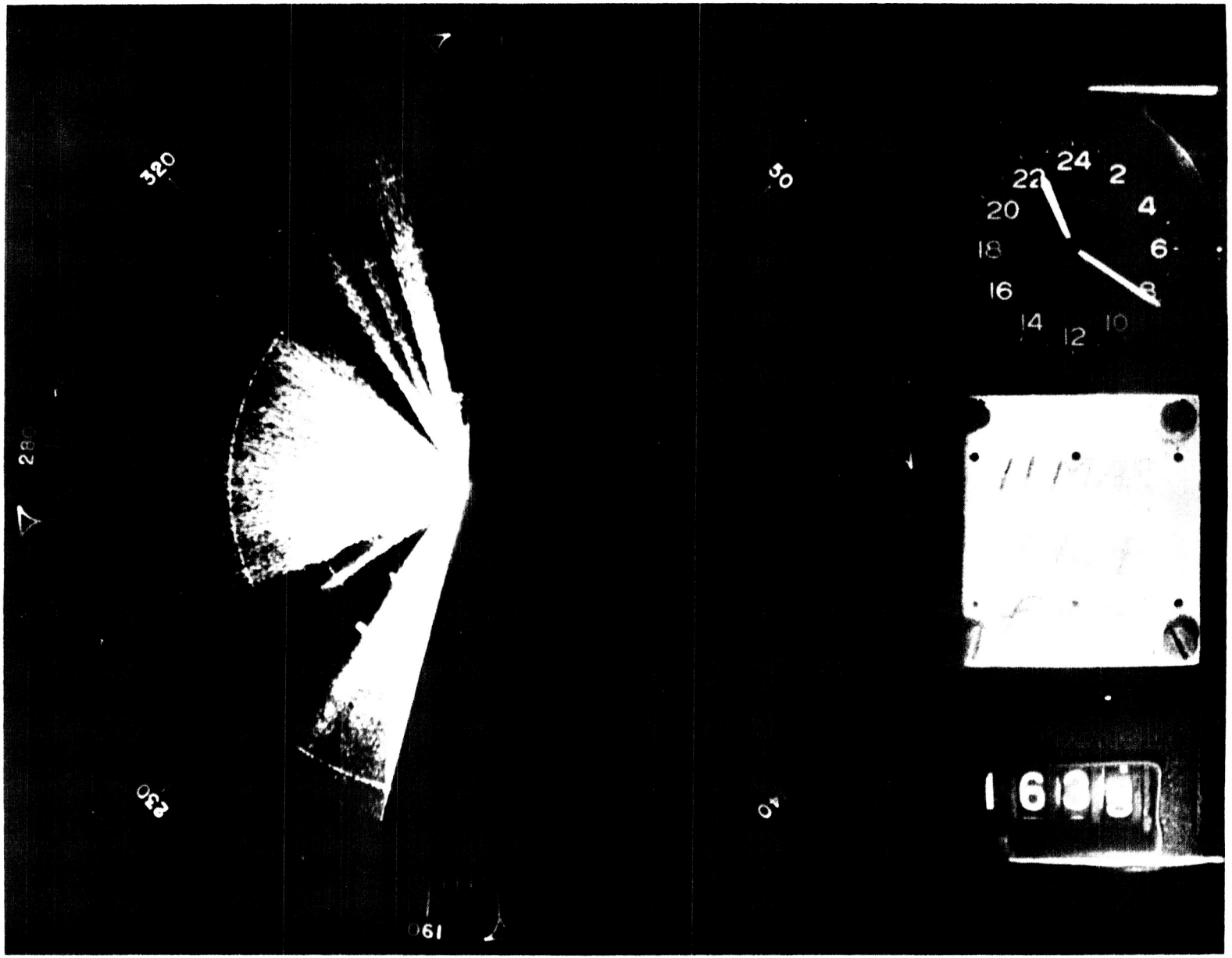

FIG. 10 CONTINUOUS PRECIPITATION AS SEEN ON PPI RADAR DISPLAY, 2220 PST, 11 MARCH 1964

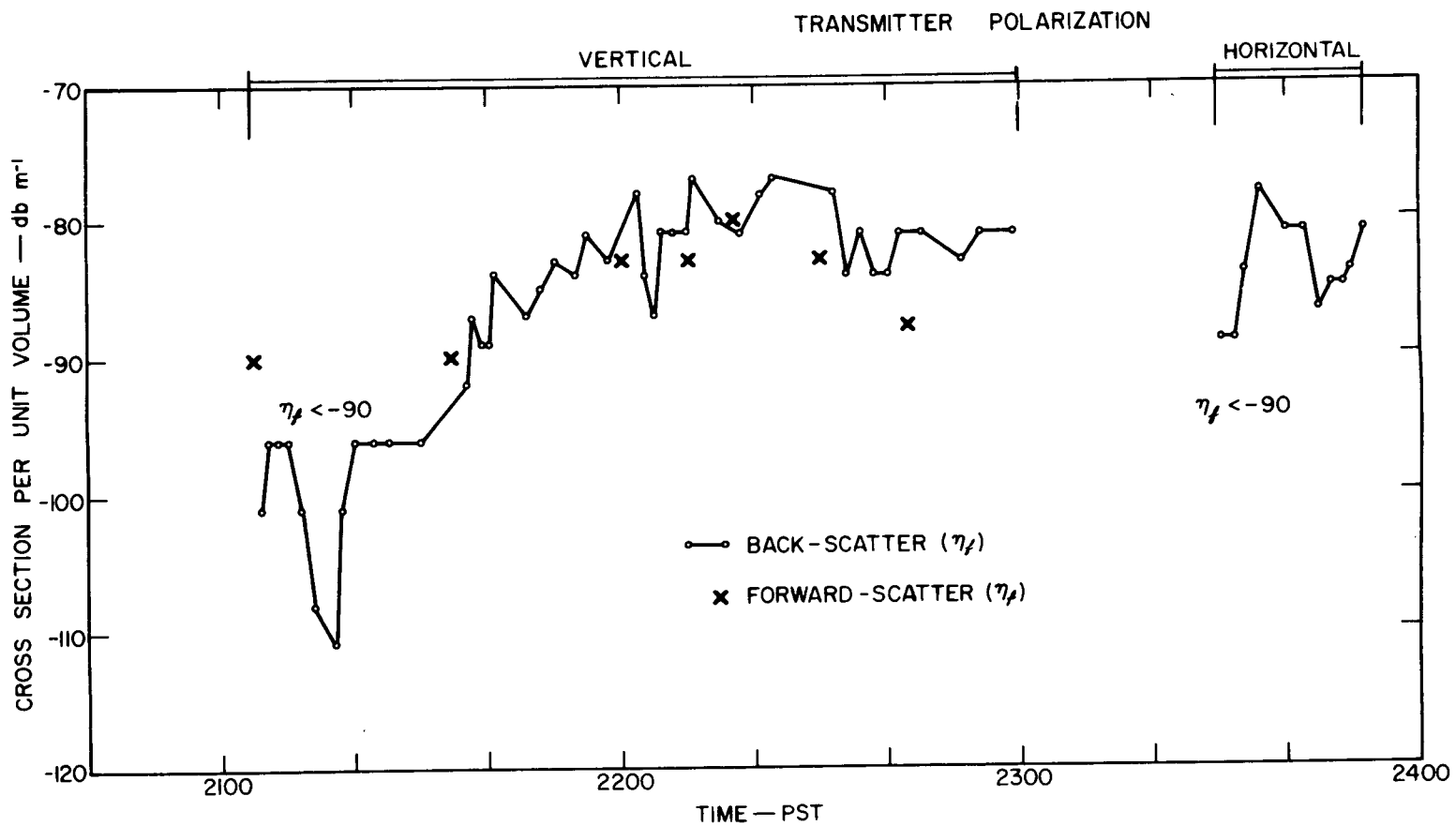

FIG. 11 CALCULATED CROSS SECTIONS PER UNIT VOLUME, 11 MARCH 1964

cross sections are based on observations of an A-scope display of the output of the radar receiver, read at 9-km range on a bearing of 291°. The back-scatter cross sections are representative of the region near the middle of the common volume, rather than of the average conditions in the common volume. Up to 2130 PST, patchy precipitation at the edge of the main precipitation shield was drifting across the propagation path. It is not surprising, therefore, that η_b and η_f varied somewhat independently of each other during this period. The main shield of precipitation, of which a part is shown in Fig. 10, moved in from the west, reaching the common volume about 2130 PST and the transmitter site by 2200 PST. As Fig. 11 indicates, η_b and η_f were equal after 2130 PST, within the limits of experimental error, while vertical polarization was used. With horizontally polarized transmissions, the forward-scatter signal was too weak to permit any measurements.

Another series of observations was carried out on the morning of 12 March. Wet snow fell at the transmitter site throughout the morning. The bright band extended from about 0.7 to 1.1 km above sea level, and so was entirely below the common volume.

Vertically polarized signals were transmitted from 0945 to 1030 PST. The computed values of η_b for this period ranged from -85 to -91 db m^{-1}. The transmitter beam was scanning for most of this period. The peaks of the signal wedges (see Sec. III-C-3) corresponded to values of η_f in the range -77 to -88 db m^{-1}. It is likely that the peaks are exaggerated by the fluctuating nature of the signal, and it would not be reasonable to draw any conclusions concerning the ratio of η_f/η_b from these records.

Horizontally polarized signals were transmitted from 1043 to 1115 PST. By then, the precipitation in the common volume had eased off and become somewhat variable. Computed values for η_b ranged from -88 to -97 db m^{-1}. No signals were detected at the remote receiver.

5. Storm of 22-23 March 1964

This was an unseasonably cold storm. The precipitation at the transmitter site was in the form of snow throughout, and there were several periods of wet snow at the remote-receiver site (elevation 660 m) on the morning of 23 March. All forward-scatter signals recorded must have been scattered from dry snow above the melting layer.

The photographs of the oscilloscope display at the remote receiver site were overexposed and not suitable for analysis. Some difficulty was experienced with the AFC unit in the radar receiver during operations on the evening of 22 March, so that little confidence can be placed in determinations of η_b made on that date.

The observations of the monitor scope at the remote-receiver site served to confirm the results from the storm of 11-12 March. With the radar transmitting vertically polarized signals, the signals recorded corresponded to values of η_f ranging from -71 to -76 db m^{-1}. Reference to Fig. 1 shows that these correspond, at the frequency used, to light to moderate snow. It is possible, though, that the observer tended to record the higher spikes of the fluctuating scatter signal and that the true values of η_f were a few decibels lower. Horizontally polarized signals were transmitted between 2243 and 2310 PST. They were not detected at the remote receiver, although the radar indicated that snow was still falling through the common volume.

On 23 March, 14 feet of the coaxial cable linking the remote receiver to its antenna were replaced by waveguide. Test-set measurements showed that this resulted in a 10-db improvement in system performance.

The transmitter was turned on with horizontal polarization at 1620 PST. This was near the end of the storm, and precipitation along the path had dwindled to a few irregular patches. However, with the improved performance, it was possible to identify the cross-polarized scatter signal around 1645 PST. It was weak, with the strongest individual pulses on a fast-sweep display indicating η_f at

roughly -100 db m^{-1}. The computed values of η_b for the period ranged up to -85 db m^{-1}.

The transmitter polarization was changed back to vertical at 1745 PST and the transmitter operated until 1810 PST. The forward-scatter signal was present most of the time, but, in the absence of usable photographic records, a detailed analysis of the signals does not appear to be justified.

6. Storm of 31 March-1 April 1964

This storm began on the evening of 31 March and lasted until the following afternoon. At the start, the 0°C isothermal layer was near 1.8 km above sea level. Reference to Fig. 7 indicates that the bright band extended downward into the common volume at that time, but that the precipitation was completely melted to rain before reaching the base of the common volume. Temperatures at the surface and aloft fell gradually throughout the storm period, with the 0°C level dropping to 1.4 km by the end. The bright band was by then occupying the lower part of the common volume, and extending perhaps 200 m below its lowest part. Thus, conditions were suitable for measurements of bright-band scattering throughout the storm.

Figure 12 is an example of the forward-scatter signals recorded on the evening of 31 March with the transmitter beam pointed at the remote receiver. At the writing speed used (1 cm/sec), the individual pulses are not resolved. The spot on the face of the tube rose and fell 333 times per second, too rapidly for the sides of the pulses to register on the photographic film. The line that appears is the envelope of the tops of the pulses. The fluctuations in it are due to shuffling of the particles contributing to the received signal.[15]

The mean signal intensity can be derived from records of the form of Fig. 12 by noting the frequency with which the instantaneous value exceeds a suitably chosen threshold.[15] If the threshold be denoted by H and the mean intensity by $\overline{P}_{rr}$, and if $\underline{p}$ instantaneous values out of k exceed H, then the best estimate of $\overline{P}_{rr}$ is given by

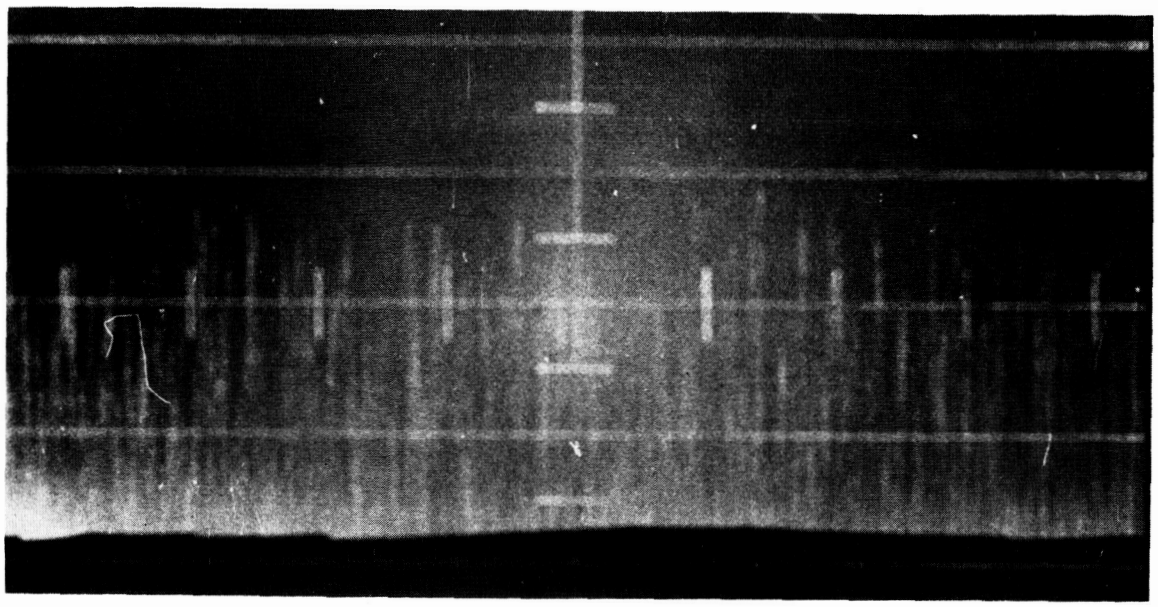

FIG. 12 FORWARD-SCATTER SIGNALS FROM THE MELTING LAYER, 2323 PST, 31 MARCH 1964 (antennas fixed)

$$\tilde{P}_{rr} = \frac{H}{\log_e (k/p)} \quad . \tag{12}$$

The distribution of $\tilde{P}_{rr}$ about $\overline{P}_{rr}$ is a function of the number of statistically independent samples of the signal used and of the ratio $H/\overline{P}_{rr}$. In the analysis of the data of 31 March-1 April, 100 instantaneous values taken at 50-msec intervals have been used in each determination of $\tilde{P}_{rr}$. Figure 7 of Ref. 15 shows that the root mean square of the ratio $\tilde{P}_{rr}/\overline{P}_{rr}$, expressed on a logarithmic scale, is near 1 db for such a sample, provided that the instantaneous values are statistically independent.

The autocorrelation of the forward-scatter signals over 50-msec intervals has been derived by a study of the frequency of threshold crossings in the samples[16] used to derive $\tilde{P}_{rr}$. The results show autocorrelation coefficients ranging from 0.1 to 0.7. The relatively high autocorrelation, compared to that of back-scatter signals,[16] is due to the path geometry: for a scatterer on the direct path between the two antennas, there is no motion possible which can change the total length

of the path from transmitter to scatterer to receiver [see Eq. (8)]. Because of the partial correlation, the samples used are not equivalent to 100 independent data each, so that the standard error of estimate of the computed value of $\overline{P}_r$ is somewhat greater than 1 db. However, since it is likely that measurement and calibration errors amount to upwards of 5 db, the samples can be regarded as adequate for present purposes.

Figure 13 shows the results for the late evening of 31 March and for 1 April. The radar indicated rather uniform precipitation in

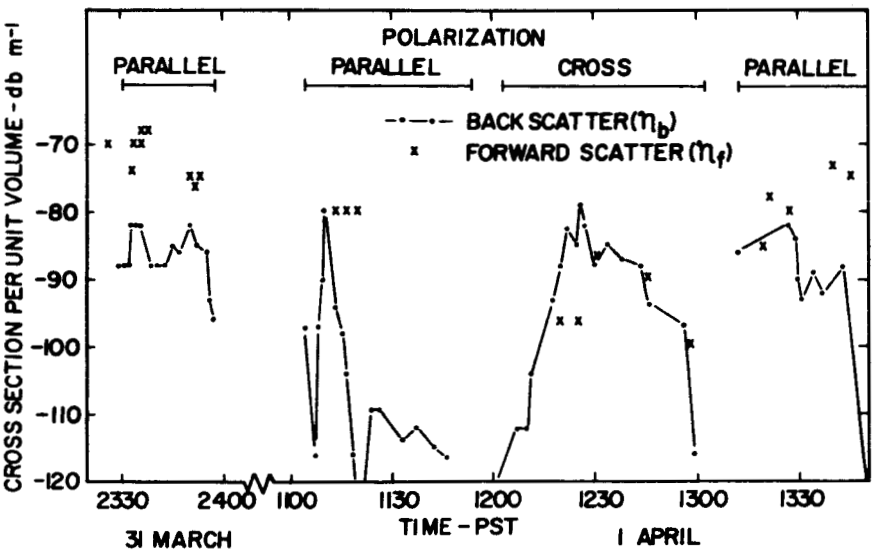

FIG. 13 CALCULATED CROSS SECTIONS PER UNIT VOLUME, 31 MARCH-1 APRIL 1964

the common volume during the evening of 31 March, and this is borne out by the relatively small variations in η_f and η_b. The noteworthy feature of these results is the fact that η_f consistently exceeds η_b by 6 to 15 db. Some experimental error is undoubtedly present, but it is worth recalling that observations on dry snow during earlier storms showed η_f and η_b to be approximately equal. It is concluded, therefore, that the apparent excess of η_f over η_b is real; that is, the scattering of C-band radiation by wet snowflakes is predominantly forward, at least in this case.

During the first period of operation on 1 April, from 1104 to 1152 PST, numerous small showers were present along the path. The value of η_f remained quite steady, however, since the common volume was large enough to hold several of the precipitation cells simultaneously (Fig. 14). The results indicate that scattering was again mainly in the forward direction. If it had been isotropic, η_b would have risen much higher than η_f at 1110 PST, when one of the showers drifted through the middle of the common volume. As it was, the predominance of forward scattering was sufficient to offset the dilution of η_f by averaging over a common volume only partially filled with precipitation.

During the second period of operation, a large shower of moderate intensity drifted over the area and occupied the common volume for almost an hour. It is likely that some small hail was formed in this shower, so that the signal from the common volume cannot be ascribed entirely to melting snowflakes. The forward-scatter cross section, measured for the cross-polarized component, was generally 5 to 10 db below η_b. Assuming that the ratio η_f/η_b would have been at least unity for vertically polarized transmissions, it is seen that polarization diversity can be quite effective in suppressing unwanted scatter signals, even when the scatterers are of irregular shape.

Another moderate shower spread across the common volume shortly after 1300 PST. It is estimated that by then the true bright band was limited to the lower half of the common volume, although wet hail was probably present throughout the common volume. The transmitter was operated with vertical polarization starting at 1313 PST. The function η_f was generally greater than η_b, with its mean at 1340 PST estimated at -72 db m^{-1}, 18 db greater than η_b at that time. The even-larger ratios of η_f/η_b after 1343 PST occurred after the trailing edge of the shower had passed the middle of the common volume, and so do not give a true picture of the scattering pattern. Clearing conditions set in behind the shower, and the equipment was turned off at 1415 PST.

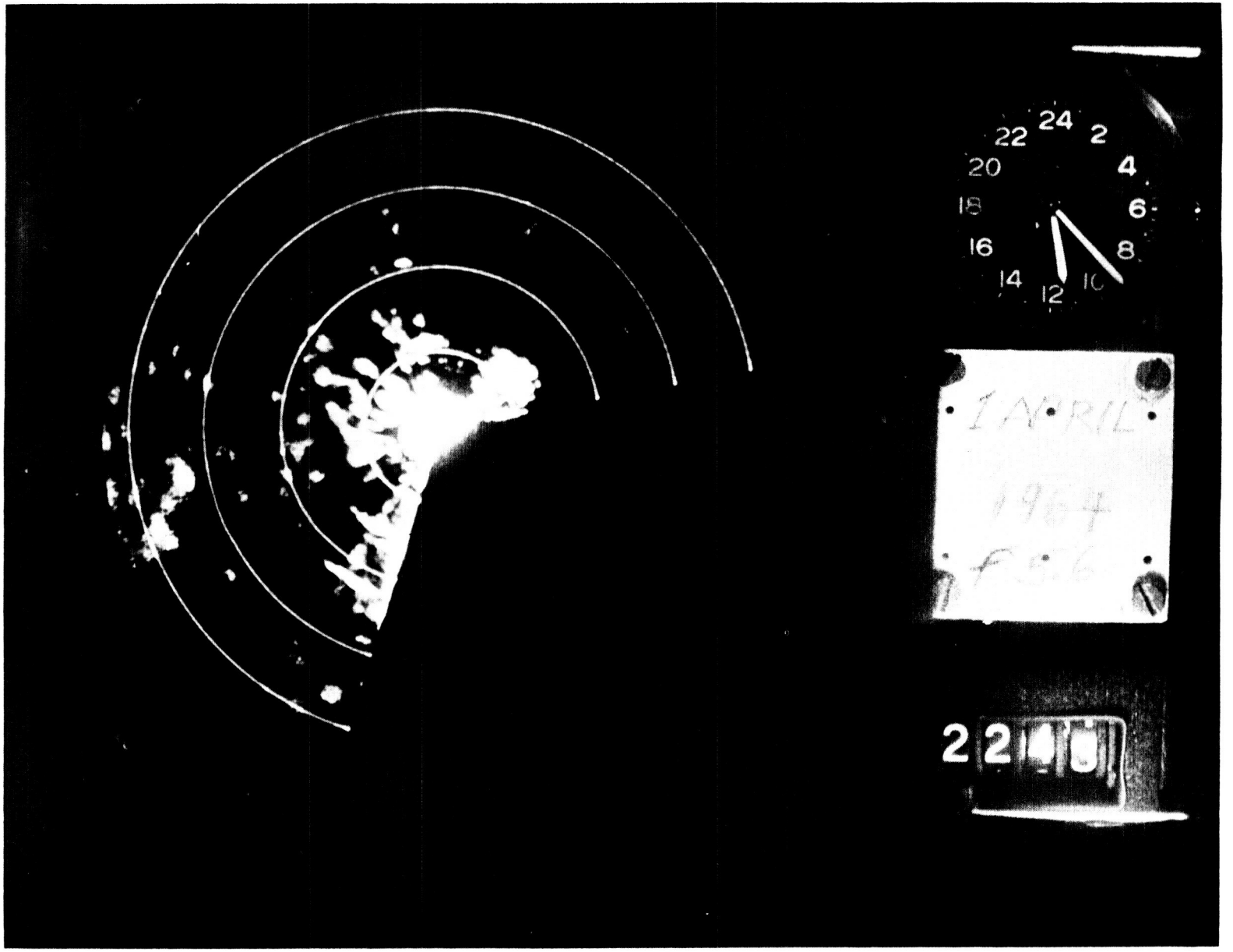

FIG. 14 SMALL SHOWERS AS SEEN ON PPI RADAR DISPLAY, 1123 PST, 1 APRIL 1964

D. SUMMARY OF RESULTS

The values of η_f and η_b found in this experiment are consistent with the results from the field of radar meteorology, as well as with each other. The largest values of η_b, in the range from -77 to -82 db m^{-1}, correspond to light-to-moderate rain or snow (Fig. 1).

The observations of scattering by dry snowflakes can be explained on the basis of Rayleigh scattering theory. The forward- and back-scatter cross sections, η_f and η_b, are approximately equal when the transmitting and receiving antennas are aligned in terms of polarization. A cross-polarized component is sometimes present, but it is weak.

Where the scattering is due to wet snowflakes or hail, the more rigorous Mie theory must be used. The function η_f can then be as much as 10 to 15 db above η_b, reaching values in the neighborhood of -70 db m^{-1} for C-band signals. This occurs with the polarization of the two antennas aligned.

The cross-polarized component of forward scatter is much stronger for wet snow than for dry snow. The function η_f, computed for the cross-polarized component, has been observed to equal η_b in a case with scattering from the melting layer of a moderate shower. It is likely that η_f for the parallel-polarized component was larger than η_f (cross-polarized) and η_b in this case, so that this result in no way rules out the potential value of polarization diversity in suppressing unwanted scatter signals.

IV GENERAL DISCUSSION

Both the Central Radio Propagation Laboratory experiment on scattering by hail in Colorado and the experiment on scattering by wet snow in California have provided evidence of Mie (i.e., non-Rayleigh) scattering of SHF radio waves.

The evaluation of the importance of precipitation scatter as an interference source in communication systems using satellites and in other SHF systems, such as search radars, will require climatological studies in addition to field experiments.

As precipitation is generally limited to a small fraction of the earth's surface at any one time, precipitation-scatter effects will be of importance in determining the interference levels to be expected 0.1% of the time, 1% of the time, and so on, rather than median interference levels. However, these probability levels are precisely those which engineers studying service reliability are most likely to consider crucial.

The effective cross-sections encountered in practice will generally be averages over extensive regions of the atmosphere, and so will correspond to light rain or snow, rather than to heavy rain, hail, or melting snow, which tend to be limited in horizontal or vertical extent. Such averaging of η_f has been noted in some of the situations described in this report. On the other hand, the averaging will tend to increase the fraction of the time that a particular link is subject to this form of interference. Second-order statistics, on the spatial extent of precipitation areas, are needed to assess this averaging effect.

The second-order statistics would also show the probability of 2 stations being simultaneously affected by precipitation scatter as a function of the distance between them. Thus, they would permit a calculation of the improvement in reliability possible through the use of space diversity.

The ranges to which precipitation-scatter interference can reach depend upon the vertical extent of the precipitation. Therefore, the climatological studies mentioned above should consider three-dimensional precipitation patterns rather than surface conditions only. Unfortunately, the available weather radar records suitable for this purpose are not extensive, and only a small amount of data has been compiled. Examination of existing records shows that precipitation more than 6 to 8 km above sea level is generally restricted to convective cells, which occupy only a small fraction of a representative area (say, 10^4 km^2) at a time.[17] This indicates that most precipitation scatter effects occur at ranges under 300 km, for antennas on the ground. However, when 99.9-percentile levels are of importance, as in satellite communication, no conclusions concerning any propagation path can be drawn without a detailed study of storm statistics for that particular area.

ACKNOWLEDGMENTS

The writer wishes to acknowledge the helpful supervision of Mr. Ronald T.H. Collis, Head of the Radar Aerophysics Group at Stanford Research Institute, throughout the course of the work covered in this report. Mr. George E. Davis, Senior Electronics Technician deserves credit for the successful equipment modifications described in Sec. III-A and for the relatively trouble-free field operations. The contribution of Mr. Albert Smith, Meteorologist, to the field operations is also worthy of special notice.

Thanks are extended to E. R. Brunette Electronics for the provision of laboratory space at Columbia Airport and to Mr. Ernest Muller, upon whose property the radar set was located.

REFERENCES

1. W. E. Gordon, "A Comparison of Radio Scattering by Precipitation and by a Turbulent Atmosphere," Proc. Third Weather Radar Conf., pp. F17-F24, McGill University, Montreal, Quebec (September 1952).

2. L. H. Doherty and S. A. Stone, "Forward Scatter from Rain," Trans. IRE, PGAP-8, pp. 414-418 (July 1960).

3. "Frequency Allocations for Space Communications," a report of the Joint Technical Advisory Committee of the Institute of Radio Engineers and the Electronic Industries Association (March 1961).

4. A. S. Dennis, "Forward Scatter from Precipitation as an Interference Source at Stations Monitoring Satellites," Research Memorandum 2, Contract NASr-49(02), SRI Project 3773, Stanford Research Institute, Menlo Park, California (November 1961, revised).

5. A. S. Dennis, "Measurements of Forward Scatter from Rain at 9.05 Gc," Research Memorandum 4, Contract NASr-49(02), SRI Project 3773, Stanford Research Institute, Menlo Park, California (May 1962).

6. K. L. S. Gunn and T. W. R. East, "Microwave Properties of Precipitation Particles," Quart. J. Roy. Meteor. Soc., 80, pp. 522-545 (October 1954).

7. K. L. S. Gunn and J. S. Marshall, "The Distribution with Size of Aggregate Snowflakes," J. Meteor. 15, pp. 452-461 (October 1958).

8. L. J. Battan, Radar Meteorology, pp. 85-90 (University of Chicago Press, 1959).

9. B. M. Herman and L. J. Battan, "Calculations of the Total Attenuation and Angular Scatter of Ice Spheres," Proc. Ninth Weather Radar Conference, Kansas City, Missouri, October 1961, pp. 259-265 (American Meteorological Society, Boston, Massachusetts).

10. D. Atlas, M. Kerker, and W. Hitschfeld, "Scattering and Attenuation by Non-Spherical Atmospheric Particles," J. Atmos. and Terrest. Phys., Vol. 3, pp. 108-119 (1953).

11. R. E. Newell, S. G. Geotis, M. L. Stone, and A. Fleisher, "How Round Are Raindrops?," Proc. Fifth Weather Radar Conf., pp. 261-268 (Signal Corps Engineering Laboratories, 1955).

12. R. Wexler, "An Evaluation of the Physical Effects in the Melting Layer," Proc. Fifth Weather Radar Conf., pp. 329-334 (Signal Corps Engineering Laboratories, 1955).

13. G. H. Hagn, A. S. Dennis, R. G. Gould, and H. A. Turner, "Determination of Conditions for Multiple Use of Frequency Allocations for Satellite Communications and Ground Services," Final Report, Contract NASr-49(02), SRI Project 3773, Stanford Research Institute, Menlo Park, California (February 1963).

14. A. S. Dennis and F. G. Fernald, "A Preliminary Analysis of Forward-Scatter Signals from Showers," Research Memorandum 5, Contract NASr-49(02), SRI Project 3773, Stanford Research Institute, Menlo Park, California (October 1963).

15. J. S. Marshall and W. Hitschfeld, "Interpretation of the Fluctuating Echo from Randomly Positioned Scatterers: Part I," Canadian J. Physics, 31, pp. 962-995 (1953).

16. W. Hitschfeld and A. S. Dennis, "Measurement and Calculation of Fluctuations in Radar Echoes from Snow," Scientific Report MW-23, Contract AF 19(122)-217, McGill University, Montreal, Quebec (July 1956).

17. P. M. Hamilton and K. L. S. Gunn, "Areal Integration of Precipitation Observed by Radar," Proc. Ninth Weather Radar Conference, Kansas City, Missouri, October 1961 (American Meteorological Society, Boston, Massachusetts).

STANFORD
RESEARCH
INSTITUTE

MENLO PARK
CALIFORNIA

Regional Offices and Laboratories

Southern California Laboratories
820 Mission Street
South Pasadena, California 91031

Washington Office
808–17th Street, N.W.
Washington, D.C. 20006

New York Office
270 Park Avenue, Room 1770
New York, New York 10017

Detroit Office
1025 East Maple Road
Birmingham, Michigan 48011

European Office
Pelikanstrasse 37
Zurich 1, Switzerland

Japan Office
Nomura Security Building, 6th Floor
1–1 Nihonbashidori, Chuo-ku
Tokyo, Japan

Retained Representatives

Toronto, Ontario, Canada
Cyril A. Ing
67 Yonge Street, Room 710
Toronto 1, Ontario, Canada

Milan, Italy
Lorenzo Franceschini
Via Macedonio Melloni, 49
Milan, Italy